



9th International Masonry Conference 2014 in Guimarães

Analysis of masonry walls subjected to high strain rate out-of-plane loads with a rate dependent interface model

SEYEDEBRAHIM HASHEMI RAFSANJANI¹, PAULO B. LOURENÇO², NUNO PEIXINHO³

ABSTRACT: Masonry is a composite material composed of individual units laid in and bound together by mortar. Appropriate Understanding of masonry material properties results in secure and efficient protection and strengthening of historical structures. Due to high computation costs and difficulties deal with detailed modelling of masonry structures, few studies are available in open literature dedicated to micro numerical modelling of masonry structures subjected to blast loading. In present study, the objective is to propose a dynamic interface model obeying non-associated flow rule with high strain rate effects to apply as material model for interface elements. In order to introduce the strain rate effects of brick and mortar properties, a recent developed model is applied here. Verifying the capability of the model proposed, numerical simulations are carried out to investigate the behaviour of unreinforced brick masonry walls subjected to explosive blast loading by using the finite element (FE) code ABAQUS. The results obtained are compared with field test data to find good agreement. A comprehensive parametric analysis is finally accomplished with different main material properties to evaluate the effect of each parameter on high strain rate response of masonry walls.

Keywords: Masonry wall, low velocity impact, Interface model, Out-of-plane behaviour, Dynamic Increase factor

1. INTRODUCTION

In recent decades, a great deal of effort has been made to think out solutions to reduce destructive damages and casualties due to devastating loads such as blast loads and impact. Needless to say, masonry structures are usually vulnerable to explosive blast loads. In this regard, conducting experiments along with numerical studies leads to a better understanding of the blast response of masonry walls and the relevance of the different masonry material properties, which, consequently, results in innovation of strengthening techniques and of assessment and design methods.

A series of experimental studies in masonry panels and structures has been carried out to report their blast response, including maximum deflection and failure mechanisms of collapse, and to evaluate their performance. Varma et al. [3] provided the 27 full scale tests on brick panels with different thickness subjected to blast loading, and reported the blast responses including the maximum deflection, the damage level, the reflected pressure, and the reflected impulse. Evaluation of structural masonry damage and fragmentation of non-retrofitted masonry walls has also been of interest in a number of studies. The crack patterns of unreinforced masonry walls subjected to low

¹ Ph.D candidate, ISISE, Civil Engineering department, University of Minho, b6000@civil.uminho.pt

² Professor, ISISE, Civil Engineering department, University of Minho, pbl@civil.uminho.pt

³ Assistant professor, CT2M, Mechanical Engineering department, University of Minho, Peixinho@dem.uminho.pt

velocity impacts were classified into two groups based on the time of formation in Gilbert, Hobbs, and Molyneaux [2]. Eamon, Baylot, and O'Daniel (6) [4] classified the CMU wall behavior against blast loads into three categories, using different ranges of pressure magnitude namely high, moderate and low.

Due to the costs of laboratory tests, it is impossible to carry out a large number of tests. Currently, given the development of computer technology, it is easy to have more detailed and accurate predictions, including dynamic response and localized damage through numerical simulations. Two common strategies have been developed for numerical simulation of masonry in the literature, namely micro strategy and macro strategy, see e.g. Lourenço [1]. Using the micro approach, a more accurate representation of the behavior of a masonry structure is usually obtained with detailed failure mechanisms of the components, while, in a macro approach, the global behavior of the structures is usually of more concern. Within, the macro approach, homogenization techniques incorporate the geometry at micro-level and became rather popular in the last decades, see Lourenço et al. [5] for a review. Depending upon the required accuracy, reliability, availability and computational costs, one of the approaches can be selected.

Recently, a numbers of investigations have been performed to identify and determine relevant parameters for blast response of masonry walls. A parametric study was conducted by Wei and Stewart [6] to study the influence of mortar and brick strength, boundary conditions and wall thickness on response of the wall. As expected, increasing the mortar or brick strength decreases the maximum deflection of the wall. Also, an increase in the number of the fixed edges or wall thickness causes a reduction in the maximum deflection of the wall.

In present paper, a newly developed dynamic interface model that includes non-associated flow rule and high strain rate effects is proposed for numerical simulations of the structural response of masonry walls subjected to low velocity impact using the finite element (FE) code ABAQUS. A micro approach is used for numerical modeling of masonry walls. The developed model is attributed to interface elements to simulate the mortar behavior between two boundaries. A comparison between numerical results and field test data obtained by Gilbert et al. [2] is performed to evaluate the performance of the proposed material model and the accuracy of the simulation in predicting the impact response and damage of masonry walls. Finally, a parametric study is carried out to discuss the effectiveness of the main parameters changes on the global behavior of masonry walls.

2. A DYNAMIC INTERFACE MODEL FOR HIGH STRAIN RATES

Recently, a series of investigations has been conducted to derive constitutive models for different materials subjected to high strain rate loading. A plastic damage material model was introduced to characterize the brick and mortar behavior in micro numerical simulation of blast response of unreinforced walls by Wei and Stewart [6]. The damage dependent piecewise Drucker-Prager strength criterion was adopted for continuum modeling of brick and mortar. A simple rigid-perfectly plastic homogenization masonry model was proposed by Milani, Lourenço, and Tralli [7] for micro numerical simulation of masonry structures subjected to out-of plane high strain rate loads. The proposed model is characterized by a low number of input material parameters, and also by being numerically inexpensive and robust. The aforementioned model was assigned to a FE thin plate triangular element.

A rate dependent interface model is introduced here to characterize the mortar behavior. Depending upon the main failure mechanisms of masonry walls, the failure envelop is divided into three parts namely, tension cut-off, Coulomb friction, and elliptical cap, see Fig. 1. Hence, each part has its own failure criterion presented in terms of k , where the k parameter is a scalar involved to measure the amount of softening and hardening in order to control the yield surface, and in terms of the stress $\boldsymbol{\sigma}$. For a 3D configuration, $\boldsymbol{\sigma} = \{\sigma, \tau_s, \tau_t\}^T$, $D = \text{diag}\{k_n, k_s, k_t\}$ and $\boldsymbol{\varepsilon} = \{\Delta u_n, \Delta u_s, \Delta u_t\}^T$. The subscripts n , s , t denote the normal and two perpendicular shear components.

In order to consider the high strain rate effects on the interface material model, a few number of dynamic increase factors (DIFs) are defined to control the failure envelop. The DIF is the ratio

between the dynamic and static parameters' values. These factors multiply the material parameters to expand or to contract the failure envelope at different strain rate levels.

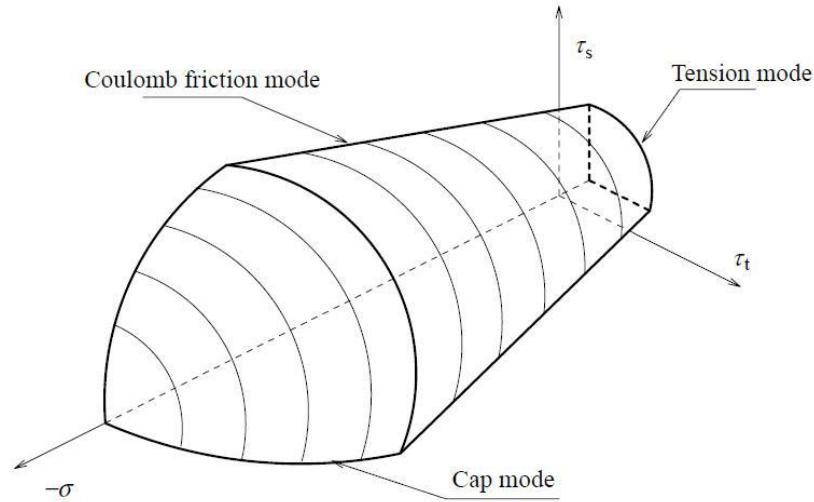


Figure 1. 3D Failure envelope of the interface cap model [1].

For the tension cut-off mode, the yield function is given as follows

$$f_1(\sigma, k_1) = \sigma - f_t \exp\left(-\frac{f_t}{G_f^I} k_1\right) \quad (1)$$

where σ denotes the normal stress and k_1 denotes a scalar to measure the amount of softening. f_t is the tensile strength of the joint (usually equal to the unit-mortar interface) and G_f^I is the mode I fracture energy.

The dynamic increase factors are applied to the uniaxial tensile strength and the fracture energy to obtain

$$f_t = DIF \times f_{t_0} \quad (2)$$

$$G_f^I = DIF \times G_{f_0}^I \quad (3)$$

where, f_{t_0} and $G_{f_0}^I$ are the quasi-static strength and fracture energy under uniaxial tension, respectively.

As in mode I the normal plastic relative displacement governs the softening behavior, the scalar \dot{k}_1 can be assumed equal to

$$\dot{k}_1 = \dot{\lambda}_1 \quad (4)$$

Where $\dot{\lambda}_i$ is the plastic multiplier.

When yielding occurs, the plastic corrector brings back the stress update to the yield surface by applying locally a Newton-Raphson method to solve the nonlinear system and updating the stress tensor and the user-defined state variables. In a plasticity model, it is worth to mention that at the starting point the stress is assumed to be elastic (considering a trial value), such as $\sigma_{n+1} = \sigma^{trial}$, $\dot{k}_{n+1} = 0$, and $\dot{\lambda}_{n+1} = 0$, which is obtained by the elastic predictor. The unknowns of the nonlinear

system of equations that arise in this update procedure are the stress components, \dot{k}_{n+1} and $\dot{\lambda}_{n+1}$. The stress update equations are given for a finite step are given by

$$\sigma_{n+1} = \sigma^{trial} - D\dot{\varepsilon}_{n+1}^p \quad (5)$$

$$\text{with } \sigma^{trial} = \sigma_n + D\dot{\varepsilon}_{n+1}^e.$$

where $\tau = \sqrt{\tau_s^2 + \tau_t^2}$ is assumed for 3D configuration.

In mode II, the Coulomb friction yield criterion reads

$$f_2(\sigma, k_2) = \tau + \sigma \tan \phi - c \exp\left(-\frac{c}{G_f^{II}} k_2\right) \quad (6)$$

Here, τ and $\bar{\sigma}_2$ are given

$$\tau = \sqrt{\tau_s^2 + \tau_t^2} \quad (7)$$

where, c denotes the cohesion of the unit-mortar interface, G_f^{II} is fracture energy in mode II, and ϕ denotes the friction angle.

The dynamic increase factors are applied to the cohesion, and mode II fracture energy and read

$$c = DIF \times c_0 \quad (8)$$

$$G_f^{II} = DIF \times G_{f_0}^{II} \quad (9)$$

Again, here, c_0 and $G_{f_0}^{II}$ are the quasi-static cohesion and fracture energy under shear, respectively.

(10)

In terms of pure shear, the shear plastic relative displacement can be assumed to control the softening behavior as

$$\dot{k}_2 = \dot{\lambda}_2 \quad (11)$$

For the compressive cap mode, the yield function can be better provided in matrix notation form as

$$f_3(\sigma, k_3) = \frac{1}{2} \sigma^T P \sigma + p^T \sigma - (\bar{\sigma}_3(k_3))^2 \quad (12)$$

where P is the projection matrix, given by $diag\{2C_{mn}, 2C_{ss}\}$, and p is the projection vector, given by $\{C_n, 0\}^T$. Here, C_{mn} and C_n are material parameters assumed equal to 1 and 0, respectively (this provides a centered ellipsoid in the origin). Parameter C_{ss} governs the intersection of the ellipsoid with the shear stress axis. It is recommended equal to 9, Lourenço [1].

The following law is used to introduce the hardening/softening behavior of masonry under uniaxial compression:

$$\bar{\sigma}_a(k_3) = \bar{\sigma}_i + (\bar{\sigma}_p - \bar{\sigma}_i) \sqrt{\frac{2k_3 - k_3^2}{k_p - k_p^2}} \quad (13)$$

$$\bar{\sigma}_b(k_3) = \bar{\sigma}_p + (\bar{\sigma}_m - \bar{\sigma}_p) \left(\frac{k_3 - k_p}{k_m - k_p} \right)^2 \quad (14)$$

$$\bar{\sigma}_c(k_3) = \bar{\sigma}_r + (\bar{\sigma}_m - \bar{\sigma}_r) \exp\left(m \frac{k_3 - k_m}{\bar{\sigma}_m - \bar{\sigma}_r}\right). \quad (15)$$

$$\text{with } m = 2 \frac{\bar{\sigma}_m - \bar{\sigma}_p}{k_m - k_p}$$

Here, the subscripts l, m, p and r in the yield value and scalar k indicate the initial, medium, peak and residual values, respectively, providing parabolic hardening, followed by exponential softening, see Figure 2.

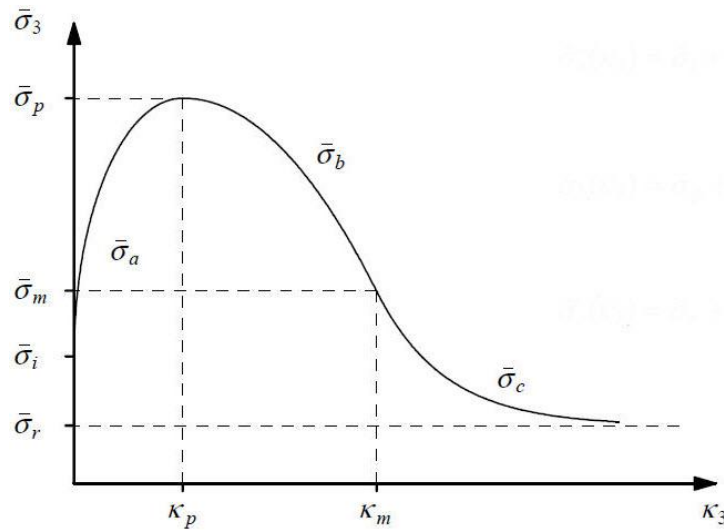


Figure 2. Hardening/softening law for cap mode [1].

The dynamic increase factors of uniaxial compressive strength and hardening are utilized to shift the failure envelop at different strain rates.

$$f_m = DIF \times f_{m_0} \quad (16)$$

$$k_m = DIF \times k_{m_0} \quad (17)$$

$$k_p = DIF \times k_{p_0} \quad (18)$$

Here, f_{m_0} , k_{p_0} , and k_{m_0} are quasi-static strength, amount of hardening corresponding to uniaxial compressive strength and scalars defining the inelastic law.

Considering an associated flow rule and strain hardening/softening hypothesis, the scalar \dot{k}_3 obtains

$$\dot{k}_3 = \dot{\lambda}_3 \sqrt{(P\sigma + p)^T (P\sigma + p)} \quad (19)$$

Hao and Tarasov [8] conducted a series of dynamic uniaxial compressive tests on brick and mortar, providing the DIFs for the material parameters at a specific range of strain rate. The derived DIFs are used in present study to characterize the materials behavior at high strain rates.

Hence, the DIF for material properties in tension, shear and compression is assumed here due to lack of report on tensile and shear material properties of masonry.

For the implementation of the proposed dynamic interface model in ABAQUS, a FORTRAN 77 user-subroutine was developed. Through this process, the material model is introduced by a failure

criterion and the adopted Euler backward algorithm (linear predictor-plastic corrector approach) in the stress update process. The user-subroutine VUINTER provided in ABAQUS is involved to define contact interface behavior. The interface material is assumed to be bonded to each of two contacting surfaces (slave and master surfaces).

3. NUMERICAL MODEL AND CAMPARISON WITH TEST DATA

The experimental data by Gilbert et al. [2] is used for validation of the developed numerical model. In their study, the unreinforced walls were subjected to low velocity impacts with different applied impulses. The wall, namely *URW* is considered here. The wall has clear size of $5.75 \times 1.15 \text{ m}$, made of concrete blocks with dimensions of $440 \times 215 \times 200 \text{ mm}$, bonded with mortar layers at bed joints and head joints, and is constructed for thickness of 200 mm . The wall was placed on 12 mm thick steel plates bolted to the strong floor and jointed to the wall using epoxy. Two stiff concrete blocks served as abutments and were constructed at the extremes of the walls. The abutments were connected to the walls using epoxy mortar, precluding the rotation at edges. It was noted that these types of bonding produce fixed boundary condition at three edges. Both abutments are assumed as rigid boundaries in numerical simulation because no serious damage was seen in them. The impact load was applied through a $400 \times 400 \times 50 \text{ mm}^3$ square steel plate at mid-height of the wall. The details of the wall and dimensions are shown in Figure 3. In numerical modelling, the applied load is modelled by a triangular load-time distribution with peak force of 90 KN reaches at 22.9 msec , respectively, see Figure 4.

Since the failure mechanisms of masonry walls subjected to high strain rate loads mostly deal with failure in joints, no serious damage is expected for the units and they were considered elastic and modeled by 3D solid elements.

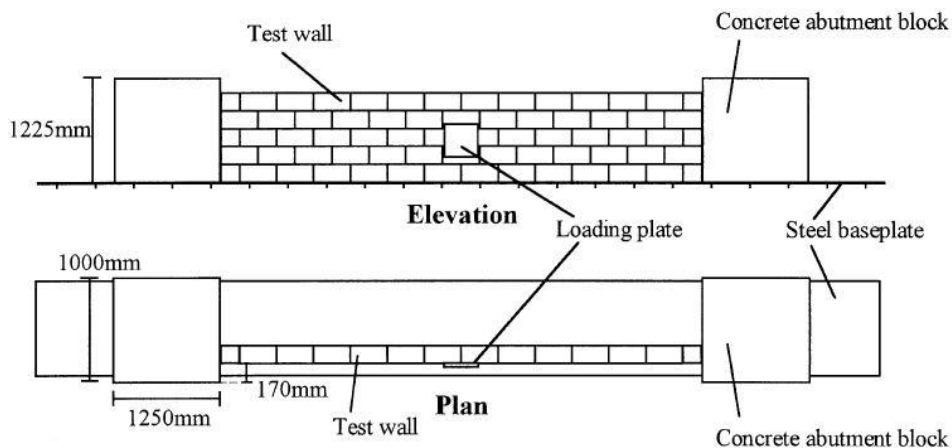


Figure 3. Geometry of masonry parapet subjected to low velocity impact [2].

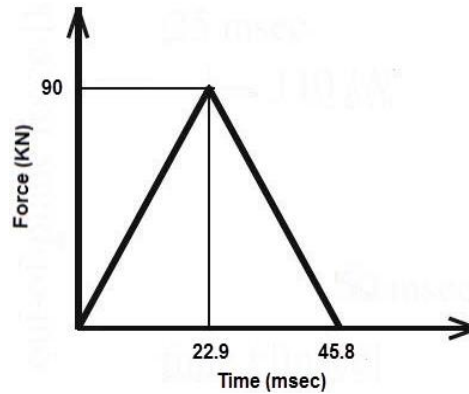


Figure 4. Typology of dynamic load applied to URW.

The finite element meshes of the wall is given in Figure 5. As shown, a fine mesh was adopted for the concrete block units. Since no field test data was reported on tensile material properties of mortar, the typical tensile material properties are adopted for the joints. The material properties of the blocks, joints and their corresponding dynamic increase factors, Hao and Tarasov [8], are presented in Table 1 and Table 2. A comparison between the predicted wall response and field test data is carried out using crack patterns and deflection, to evaluate the accuracy of the predictions. Figure 6 show the observed crack patterns of the tested parapet, URW subjected to out of plane impact load. The deformations of the parapet recorded at the maximum deflections is presented in Figure 7. According to predictions, it is noted that vertical cracks were formed over entire height of the parapet URW at the center and to each side, and both right and left parts rotated inside. Moreover, the cracks are distributed along the length of the parapet. An appropriate agreement is also noted in prediction of failure modes between the test and simulation.

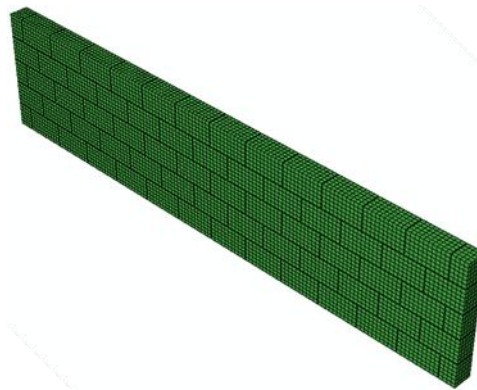


Figure 5. Finite element scheme of URW.

Table 1. Material properties of the blocks and DIFs [2, 8].

Elastic properties			
Weak concrete block		Strong concrete block	
E (N/m ²)	ν	E (N/m ²)	ν
1.65E10	0.2	2.88E10	0.2
DIF E	DIF ν	DIF E	DIF ν
1.74	1.15	1.74	1.15

Table 2. Material properties of the joints and DIFs [2, 8].

Inelastic properties										Elastic properties	
Tension		Shear				Cap					
F_t (MPa)	GFI (N/m)	c (MPa)	$\tan \phi$	$\tan \psi$	GFI (N/m)	F_m (MPa)	C_{SS}	k_m (m)	k_p (m)	K_n (N/m ³)	K_s (N/m ³)
0.043	17.2	0.083	0.5	0	400	8.6	9	0.3E-3	0.06E-3	9.26E10	5.447E10
DIF F_t	DIF GFI	DIF C	-	-	DIF GFI	DIF F_m	-	DIF k_p	DIF k_p	DIF K_n	DIF K_s
2.1	3.31	2.1	-	-	3.31	2.1	-	3.31	3.31	0.66	0.66

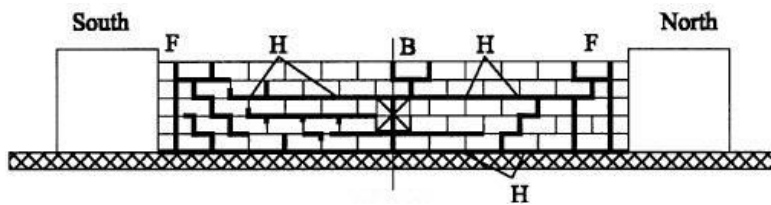


Figure 6. Observed crack patterns in test - URW[2].

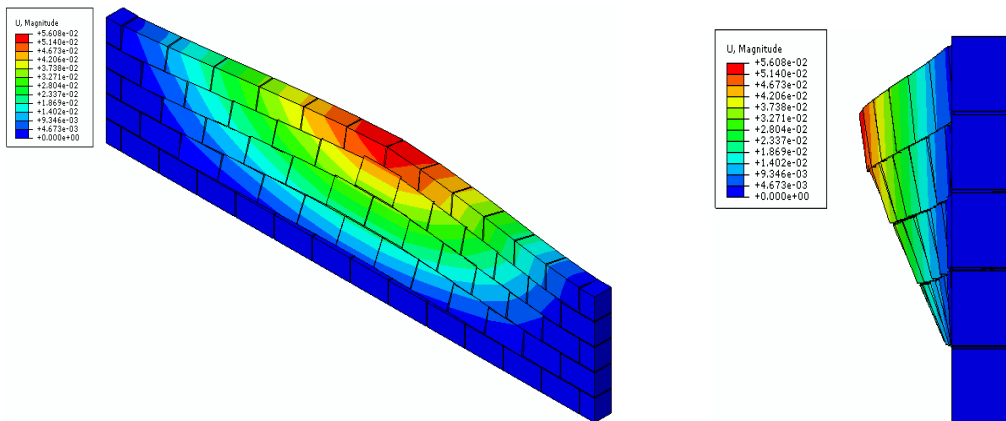


Figure 7. Deformation of URW at maximum deflection: perspective (left); side view (right)

Next, a comparison is made for the displacement vs. time response of the wall. The displacement is recorded at the point located at mid-height and 580 mm above the base, offset by 500 mm and 250 mm to the left of the centerline. As shown in Figure 8, the numerical model can predict the high strain rate response of the walls including magnitude of peak displacement and post-peak trend close to the observed test result. Here it is noted that there is a pronounced built up of stiffness found in response due to the inertial forces and acceleration of movement.

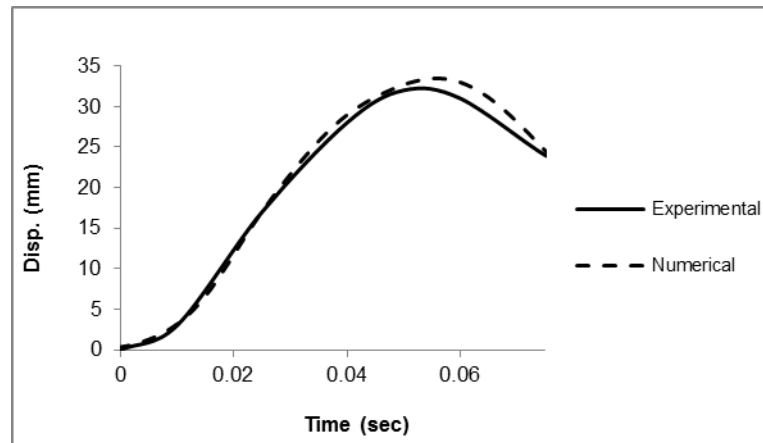


Figure 8. Displacement vs. time response of the wall URW.

4. PARAMETRIC STUDIES

The wall is involved in parametric studies to evaluate the effectiveness of the variation of the parameters, namely material properties of the joint and wall thickness, on the high strain rate response of masonry walls. The effects of the parameters are evaluated by comparing the maximum deflections and crack patterns with the reference (experimental) response.

Three types of tensile strength, and cohesion are used distinctly to investigate the effectiveness of material properties of the joint, as summarized in Table 3. Only one parameter is changed for each analysis, using Type 2 values as reference values. The displacement-time responses of the masonry wall for three types of tensile strength and three types of cohesion are presented in Figure 9 and Figure 10, respectively.

Table 3. Material properties of joints

Material parameter	Type 1	Type 2	Type 3
F_t (MPa)	0.011	0.043	0.172
c (MPa)	0.021	0.083	0.332

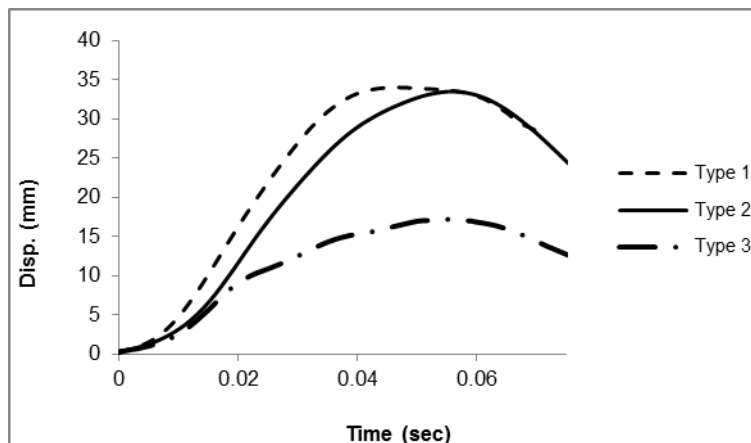


Figure 9. Displacement vs. time responses of the wall with three different types of tensile strength.

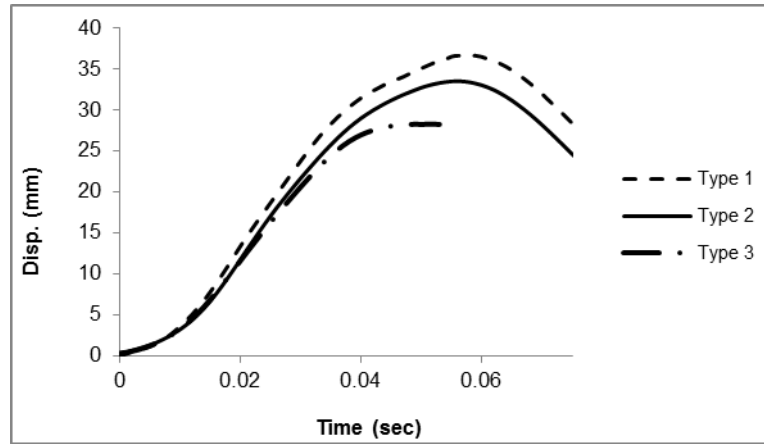


Figure 10. Displacement vs. time responses of the wall with three different types of cohesion.

Comparing the above diagrams for the masonry wall with three types of tensile strengths and cohesions, it is noted that reducing the tensile strength or cohesion leads to an increase in deflection of the wall up to 2.3 and 1.4 times, respectively. The effect of tensile strength is much larger than the cohesion for this wall. No changes could be found in the damage mechanism, so the results are not shown.

Figure 11 shows the displacement-time diagrams of the masonry wall with three wall thicknesses. The reference material properties of mortar and block are applied in the three walls. The numerical results indicate that the wall with wall thickness 200mm has the maximum deflection, as expected. The growth of deflection is almost 2.3 times with the decrease of the wall thickness. This is in opposition with a quasi-static elastic calculation, where this deformation would be proportional to the bending stiffness (in this case, this would be a maximum difference $1.5^3 = 3.4$). It is also noted that the most common used criterion for structural collapse is when the maximum deflection exceeds the wall thickness, Wei and Stewart [6], meaning that the wall with a minimum thickness of 250 mm would be required for the present load. Again, it is noted no changes could be found in the damage mechanism, so the results are not shown.

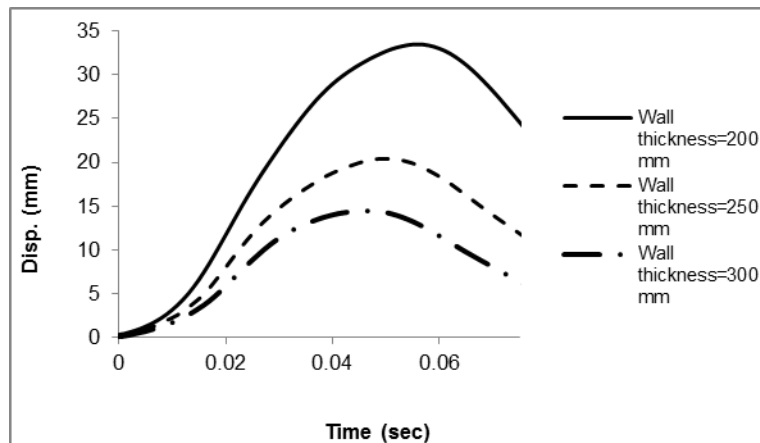


Figure 11. Displacement vs. time responses of the wall with three wall thicknesses t.

5. CONCLUSIONS

The present study aims at developing a rate dependent dynamic interface model to for the numerical simulation of masonry structures using a micro-modeling approach. The 3D interface model is implemented as a user-defined subroutine in the finite element code ABAQUS. The adequacy of the material model to replicate measured dynamic increase factors measures experimentally is demonstrated by applying various uniaxial loading conditions. A comparison between numerical predictions and field test data of two full scale masonry walls is carried out, including displacement-time response diagrams and failure mechanisms. It can be inferred from the numerical results that the model can predict the maximum deflection and failure mode over the entire length of the walls, with good agreement. Finally, a parametric study is conducted to evaluate the influence of the material properties of the joint and wall thickness on response of the walls. It is concluded that the influence of tensile strength on the maximum displacement-time response of the walls is significant, much more than the cohesion. Moreover, it was noticed that the increasing the wall thickness can decrease the maximum deflection, as expected, but the changes obtained for fast impact are significantly different than the changes in stiffness obtained in a linear elastic calculation.

REFERENCES

- [1] Lourenço P. Computational strategies for masonry structures. 1996.
- [2] Gilbert M, Hobbs B, Molyneaux T. The performance of unreinforced masonry walls subjected to low-velocity impacts: experiments. *International Journal of Impact Engineering*. 2002;27:231-51.
- [3] Varma R, Tomar C, Parkash S, Sethi V. Damage to Brick Masonry Panel Walls Under High Explosive Detonations. *ASME-PUBLICATIONS-PVP*. 1996;351:207-16.
- [4] Eamon CD, Baylot JT, O'Daniel JL. Modeling concrete masonry walls subjected to explosive loads. *Journal of engineering mechanics*. 2004;130:1098-106.
- [5] Lourenço PB, Milani G, Tralli A, Zucchini A. Analysis of masonry structures: review of and recent trends in homogenization techniques This article is one of a selection of papers published in this Special Issue on Masonry. *Canadian Journal of Civil Engineering*. 2007;34:1443-57.
- [6] Wei X, Stewart MG. Model validation and parametric study on the blast response of unreinforced brick masonry walls. *International Journal of Impact Engineering*. 2010;37:1150-9.
- [7] Milani G, Lourenço PB, Tralli A. Homogenized rigid-plastic model for masonry walls subjected to impact. *International Journal of Solids and Structures*. 2009;46:4133-49.
- [8] Hao H, Tarasov B. Experimental study of dynamic material properties of clay brick and mortar at different strain rates. *Australian Journal of Structural Engineering*. 2008;8:117.